

This is a repository copy of *Temperature and Thickness Dependence of Statistical Fluctuations of the Gilbert Damping in Co - Fe - B / Mg O Bilayers*.

White Rose Research Online URL for this paper:

<https://eprints.whiterose.ac.uk/145500/>

Version: Published Version

---

**Article:**

Sampan-A-Pai, Sutee, Chureemart, Jessada, Chantrell, Roy W. [orcid.org/0000-0001-5410-5615](https://orcid.org/0000-0001-5410-5615) et al. (5 more authors) (2019) Temperature and Thickness Dependence of Statistical Fluctuations of the Gilbert Damping in Co - Fe - B / Mg O Bilayers. *Physical Review Applied*. 044001. ISSN 2331-7019

<https://doi.org/10.1103/PhysRevApplied.11.044001>

---

**Reuse**

Items deposited in White Rose Research Online are protected by copyright, with all rights reserved unless indicated otherwise. They may be downloaded and/or printed for private study, or other acts as permitted by national copyright laws. The publisher or other rights holders may allow further reproduction and re-use of the full text version. This is indicated by the licence information on the White Rose Research Online record for the item.

**Takedown**

If you consider content in White Rose Research Online to be in breach of UK law, please notify us by emailing [eprints@whiterose.ac.uk](mailto:eprints@whiterose.ac.uk) including the URL of the record and the reason for the withdrawal request.


## Temperature and Thickness Dependence of Statistical Fluctuations of the Gilbert Damping in Co-Fe-B/MgO Bilayers

Sutee Sampan-a-pai,<sup>1</sup> Jessada Chureemart,<sup>1</sup> Roy W. Chantrell,<sup>2</sup> Roman Chepulskey,<sup>3</sup> Shuxia Wang,<sup>3</sup> Dmytro Apalkov,<sup>3</sup> Richard F. L. Evans,<sup>2,\*</sup> and Phanwadee Chureemart<sup>1,†</sup>

<sup>1</sup>*Computational and Experimental Magnetism Group, Department of Physics, Mahasarakham University, Mahasarakham 44150, Thailand*

<sup>2</sup>*Department of Physics, University of York, York YO10 5DD, United Kingdom*

<sup>3</sup>*Samsung Electronics, Semiconductor R&D Center (Grandis), San Jose, California 95134, USA*

 (Received 11 October 2018; revised manuscript received 25 January 2019; published 1 April 2019)

We theoretically investigate the temperature and thickness dependence of the effective Gilbert damping constant ( $\alpha$ ) in the Co-Fe-B/MgO system using atomistic spin dynamics. We consider a high damping constant at the interface layer and a low damping constant for the bulklike layers due to large interfacial spin-orbit coupling. We find a strong dependence of the effective Gilbert damping with the film thickness, in quantitative agreement with experimental data. The temperature dependence of the effective damping arising from thermal-spin fluctuations up to temperatures of 400 K is weak, with no apparent change over the studied temperature range. Interestingly, we find that the temperature produces a different effect: a statistical fluctuation of the Gilbert damping parameter for a given relaxation induced solely from the finite size of the system. This statistical variation of the Gilbert damping is an intrinsic effect and is important for spintronic devices operating at gigahertz frequencies, where the dynamic response must be carefully controlled.

DOI: [10.1103/PhysRevApplied.11.044001](https://doi.org/10.1103/PhysRevApplied.11.044001)

### I. INTRODUCTION

In recent years, the Co-Fe-B/MgO magnetic tunnel junction (MTJ) exhibiting high perpendicular magnetic anisotropy (PMA) has been studied extensively, since it is a promising material for applications in data-storage devices including spin-transfer torque magnetoresistive random-access memory (STT MRAM) with the requirement of high-density data storage and a high tunnel magnetoresistance (TMR) ratio [1–3]. Apart from high interfacial perpendicular magnetic anisotropy, there are a number of experimental studies reporting that Co-Fe-B possesses high thermal stability, a low critical current density for magnetization reversal, a high TMR ratio, and a relatively small damping constant [1,4–6]. For spintronic devices, it is important to understand the magnetization dynamics of magnetic materials used where the critical current density for the reversal process, the operating speed, and the power consumption are significantly related to the dynamic behavior. The speed of the dynamic behavior is characterized by the Gilbert damping parameter  $\alpha$ , which describes the dissipation of energy from the spin system to the heat bath [3,4,7,8].

For STT MRAM, the Gilbert damping parameter is particularly important, as it counteracts the effective anti-damping term induced by the spin-transfer torque (STT) and, in general, the intrinsic damping should be as small as possible to reduce the write current, enabling us to downsize an MRAM device [9]. The Gilbert damping constant is investigated as a phenomenological quantity and measured with several techniques. To obtain the Gilbert damping constant in experiments, the dynamics of the magnetization can be measured by means of a ferromagnetic-resonance (FMR) technique and then the damping constant can be given from the line-width behavior of the ferromagnetic-resonance spectrum [3,10,11]. In addition, the FMR combined with the all-optical time-resolved magneto-optical Kerr effect (TRMOKE), using a pump-probe technique, has an advantage for estimating the damping constants [7,12,13]. Theoretical first-principles calculations have predicted the damping constant in a ferromagnetic-nonmagnetic (FM-NM) system, indicating an enhancement of the damping constant with a decreasing thickness of film due to surface spin scattering [14,15].

The appropriate value of the damping constant is necessary for a theoretical investigation of magnetization reversal in Co-Fe-B/MgO/Co-Fe-B MTJs for STT MRAM applications. In this work, the temperature and thickness dependence of the effective Gilbert damping of the

\*richard.evans@york.ac.uk

†phanwadee.c@msu.ac.th

Co-Fe-B layer in the Co-Fe-B/MgO system are studied using atomistic spin dynamics. The system is modeled considering a high-anisotropy high-Gilbert-damping monolayer in contact with the MgO layer, coupled to a low-damping low-anisotropy bulk layer away from the interface. Physically, the high damping at the interface is expected to be due to the hybridization of the interfacial Fe layer, leading to a strong perpendicular interfacial anisotropy. In general, spin and lattice fluctuations are expected to contribute weakly to the Gilbert damping at temperatures significantly below the Curie and melting temperatures [16]. The spin-orbit coupling provides an energy dissipation channel for precessing spins at the interface. We note that here we only consider the isotropic part of the Gilbert damping tensor. It is known that in macroscopic experimental samples, the Gilbert damping is a tensorial quantity [17] owing to magnetic inhomogeneities. In our simulations, we simulate a small volume of the sample that is exchange dominated and so the off-diagonal components of the tensor are negligible [18]. The dynamics of the system are modeled using the stochastic Landau-Lifshitz-Gilbert (LLG) equation at the atomistic level using the VAMPIRE software package [8,19]. Subsequently, the effective damping constant is extracted from the magnetization trace. We find a strong thickness dependence and a weak temperature dependence of the effective Gilbert damping. In addition, we find a statistical variation of the Gilbert damping for a given relaxation process driven by random thermal-spin fluctuations.

## II. THE ATOMISTIC SPIN MODEL

The effective damping parameter  $\alpha$ , which is an empirical constant, can be considered from the magnetization dynamics of the magnetic layer. In order to extract the damping constant from magnetization traces, the magnetic system is modeled at the atomistic level by using the stochastic LLG equation [20], given by

$$\frac{\partial \mathbf{S}}{\partial t} = -\frac{\gamma}{(1+\alpha^2)} (\mathbf{S} \times \mathbf{B}_{\text{eff}}) - \frac{\gamma\alpha}{(1+\alpha^2)} [\mathbf{S} \times (\mathbf{S} \times \mathbf{B}_{\text{eff}})], \quad (1)$$

where  $\mathbf{S}$  is the normalized spin moment,  $\gamma$  is the absolute value of the gyromagnetic ratio,  $\alpha$  is the intrinsic damping constant, and  $\mathbf{B}_{\text{eff}}$  denotes the effective field acting on the local spin moment, which can be determined from a classical spin Hamiltonian describing the energetics of the magnetic system, written as follows:

$$\begin{aligned} \mathcal{H} = & - \sum_{i<j} J_{ij} \mathbf{S}_i \cdot \mathbf{S}_j - k_u \sum_i (\mathbf{S}_i \cdot \mathbf{e})^2 \\ & - |\mu_s| \sum_i \mathbf{S}_i \cdot \mathbf{B}_{\text{app}}, \end{aligned} \quad (2)$$

where  $J_{ij}$  is the nearest-neighbor exchange integral between spin sites  $i$  and  $j$ ,  $\mathbf{S}_i$  is the local normalized spin moment,  $\mathbf{S}_j$  is the normalized spin moment of the neighboring atom at site  $j$ ,  $k_u$  is the uniaxial anisotropy constant,  $\mathbf{e}$  is the unit vector of the easy axis, and  $|\mu_s|$  is the magnitude of the spin moment. The first term of the spin Hamiltonian represents the exchange energy. The anisotropy energy and the external applied field energy are represented in the second and third terms, respectively.

Besides the energetics of the magnetic system provided in the spin Hamiltonian, the demagnetizing field and the thermal fluctuation field should be taken into account in the model. The inclusion of the demagnetizing field is calculated separately at the micromagnetic level, using the macrocell approach to reduce the computational time [8,21]. The magnetic moment of each macrocell is determined by the summation of the atomic spins within the cell. The demagnetizing field of macrocell  $k$  containing spin  $i$  is given by

$$\mathbf{B}_{\text{dip},k} = \frac{\mu_0}{4\pi} \sum_{l \neq k} \left[ \frac{3(\boldsymbol{\mu}_l \cdot \hat{\mathbf{r}}_{kl})\hat{\mathbf{r}}_{kl} - \boldsymbol{\mu}_l}{|\mathbf{r}_{kl}|^3} \right] \quad (3)$$

and

$$\boldsymbol{\mu}_l = \mu_s \sum_{i=1}^{n_{\text{atom}}} \mathbf{S}_i, \quad (4)$$

where  $\boldsymbol{\mu}_l$  is the vector of the magnetic moment in the macrocell site  $l$ ,  $\mu_0$  is the permeability of free space,  $V$  is the volume of the macrocell,  $r_{kl}$  is the distance and  $\hat{\mathbf{r}}_{kl}$  the corresponding unit vector between macrocell sites  $k$  and  $l$ , and  $n_{\text{atom}}$  is the number of atoms in each macrocell. It is worthwhile noting that the dipole field is assumed to be constant over the cell  $k$  containing spin  $i$ .

The thermal fluctuation of the spin moments arising from the effect of temperature can be taken into account in the atomistic model using Langevin dynamics in the formalism of Brown [22], under the assumption that the inclusion of temperature can be represented by a random field term [23–27]. The introduction of the thermal fluctuations into the atomistic model enables the study of the ferromagnetic-paramagnetic transition. The statistical properties of the fluctuation field  $[\mathbf{B}_{\text{th}}^i(t)]$ , represented by a Gaussian distribution, are given by the following equations:

$$\begin{aligned} \langle \mathbf{B}_{\text{th}}^i(t) \rangle &= 0, \\ \langle \mathbf{B}_{\text{th}}^i(t) \mathbf{B}_{\text{th}}^j(t') \rangle &= \frac{2\alpha k_B T}{\mu_s |\gamma|} \delta_{ij} \delta(t-t'), \end{aligned} \quad (5)$$

where  $i$  and  $j$  are the Cartesian components,  $\mathbf{B}_{\text{th}}$  is a random field with the Gaussian fluctuations,  $2\alpha k_B T / (\mu_s \gamma)$  is the strength of the thermal fluctuations,  $k_B$  is the

Boltzmann constant,  $T$  is the system temperature in kelvin,  $\alpha$  is the damping parameter, and  $|\gamma|$  is the absolute value of the gyromagnetic ratio.

To observe the spin dynamics, including the effect of temperature in the atomistic model, the thermal fluctuation is represented by a Gaussian distribution  $\Gamma(t)$  in three dimensions, with a mean of zero. The thermal field on each spin site  $i$  at each time step ( $\Delta t$ ) can be calculated as follows:

$$\mathbf{B}_{\text{th}}^i(t) = \Gamma(t) \sqrt{\frac{2\alpha k_B T}{\gamma \mu_s \Delta t}}. \quad (6)$$

Consequently, the effective local field, which includes Zeeman, exchange, anisotropy, and demagnetization contributions and a random thermal field acting on the spin site  $i$  in the atomistic model, is given by

$$\mathbf{B}_{\text{eff},i} = -\frac{1}{|\mu_s|} \frac{\partial \mathcal{H}}{\partial \mathbf{S}_i} + \mathbf{B}_{\text{dip},k} + \mathbf{B}_{\text{th},i}. \quad (7)$$

The dynamics of the magnetization can be investigated by substituting the local effective field from Eq. (7) into Eq. (1) and then the standard LLG equation can be solved numerically by using the Heun integration scheme [8].

### III. RESULTS

In this work, we aim to study the thickness and temperature dependence of the effective damping constant in Co-Fe-B/MgO structures via atomistic calculation. Initially, we present the calculation of the precession frequency of the magnetization of a Co-Fe-B layer, which represents a useful test of the atomistic model in its prediction of the dynamic magnetic properties.

The Co-Fe-B/MgO system, with dimensions of  $20 \times 20 \times 2 \text{ nm}^3$ , is modeled considering a high-anisotropy high-Gilbert-damping monolayer in contact with the MgO layer, coupled to a low-damping low-anisotropy bulk layer away from the interface. The magnetic properties of Co-Fe-B are considered as the average of the magnetic material properties of all the elements and the nonmagnetic MgO oxide layer is not included in the simulations explicitly, as illustrated in Fig. 1. The magnetic properties of Co-Fe-B used in this paper are obtained from direct comparison with experiment [28,29] and are shown in Table I. Here, we include an enhanced interfacial exchange due to the strong hybridization at the interface [30] to obtain quantitative agreement with experimental data for the temperature dependence of the magnetization [29].

To observe the precession frequency of the magnetization in the Co-Fe-B layer at 0 K using the atomistic model, the external field ranging from 0.1 to 10 T is applied along the  $z$  direction to the structure where the initial magnetization is aligned at an angle of  $30^\circ$  in the  $y$ - $z$  plane.

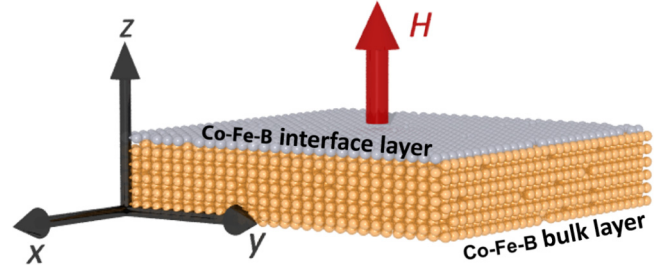


FIG. 1. A schematic of the simulated system: the white and gold spheres represent the interface layer and bulklike Co-Fe-B layer, respectively.

Figure 2 shows the dynamics of the  $y$  component of the magnetization and the precession frequency with different external magnetic fields. The relaxation time and precession frequency are evaluated by fitting the magnetization dynamics with a function given by

$$M(t) = A \exp\left(-\frac{t}{\tau}\right) \cos(2\pi ft), \quad (8)$$

where  $A$ ,  $f$ , and  $\tau$  are the amplitude of the magnetization, the precession frequency, and the relaxation time, respectively. In Fig. 2, we show that increasing the magnetic field reduces the relaxation time but increases the precession frequency of the magnetization, as expected. Our results give a good agreement with previous experimental studies [3,4]. This verifies the correctness of the atomistic model as a useful tool for further investigation of the damping in Co-Fe-B/MgO.

#### A. The thickness dependence of the effective damping

The effective damping constant, which is an intrinsic property of a material, is considered next through magnetization dynamics using the atomistic model. The Co-Fe-B system, with dimensions of  $20 \times 20 \times t \text{ nm}^3$ , is considered as a bilayer system consisting of a monolayer in contact with the MgO layer coupled to a bulk layer. To verify our approach and the correctness of the magnetic parameters of the Co-Fe-B used in this work, the thickness dependence of the effective damping at 300 K is calculated first and then compared with the previous experimental work of Ikeda *et al.* [1]. To calculate the effective damping constant of

TABLE I. The magnetic parameters of the Co-Fe-B/MgO system.

Parameters	Co-Fe-B (interface)	Co-Fe-B (bulk)
Damping constant, $\alpha$	0.11	0.003
$J_{ij}$ (J per link)	$1.547 \times 10^{-20}$	$7.735 \times 10^{-21}$
$\mu_s$ ( $\mu_B$ )	1.6	1.6
$k_u$ (J per atom)	$1.35 \times 10^{-22}$	0

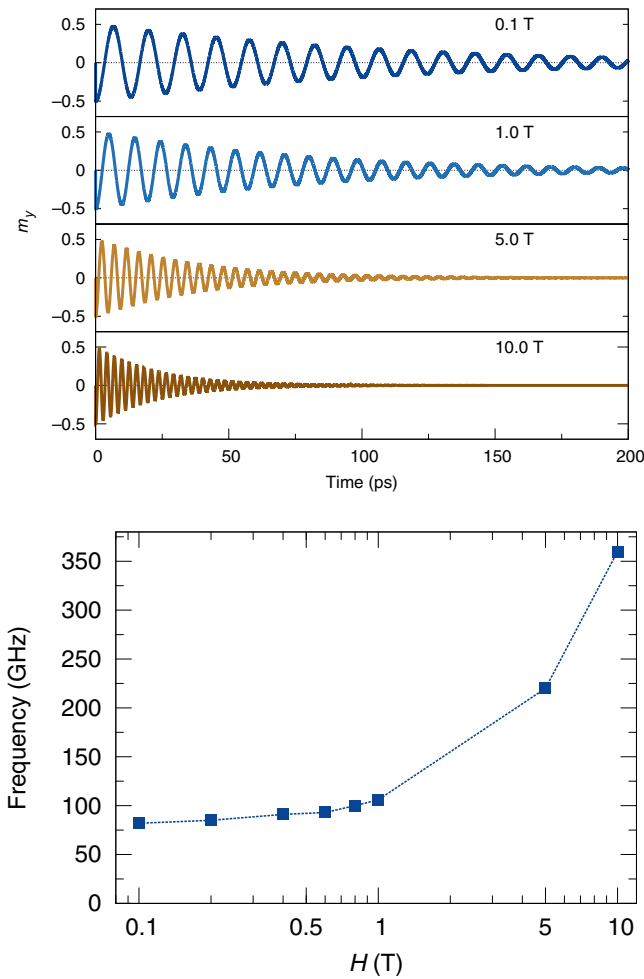


FIG. 2. The magnetization dynamics of a Co-Fe-B layer with various external fields obtained from the atomistic model (top) and the field dependence of the precession frequency of magnetization in the Co-Fe-B layer (bottom).

the Co-Fe-B system, it becomes possible to compare the magnetization dynamics obtained from simulation with the analytical solution of the LLG equation for a single spin [8,20,31,32] aligned along the  $x$  axis for a field  $\mathbf{B}$  applied along the  $z$  axis and given by

$$\begin{aligned}
 M_x(t) &= \operatorname{sech}\left(\frac{\alpha\gamma B}{1+\alpha^2}t\right) \sin\left(\frac{\gamma B}{1+\alpha^2}t\right), \\
 M_y(t) &= -\operatorname{sech}\left(\frac{\alpha\gamma B}{1+\alpha^2}t\right) \cos\left(\frac{\gamma B}{1+\alpha^2}t\right), \\
 M_z(t) &= \tanh\left(\frac{\alpha\gamma B}{1+\alpha^2}t\right).
 \end{aligned} \quad (9)$$

Simulation of the magnetization relaxation is therefore performed in order to calculate the effective Gilbert damping parameter as a function of the film thickness and the temperature. As the system has a high anisotropy, the magnetic field is a function of the  $z$  component of the magnetization.

This precludes the use of the analytical solution for a small fixed field in Eq. (9). We therefore use a large magnetic field of 10 T in the approximation  $B \gg \mu_0 H_K = 2k_u/\mu_s$  for the relaxation simulation so that the solution closely approximates the analytical solution. The system is first equilibrated with a 10 T applied field along the  $z$  axis. A uniform rotation of the thermally equilibrated spin configuration is then made to initialize the magnetization to an angle of  $30^\circ$  in the  $y$ - $z$  plane. The relaxation of the net magnetization back to equilibrium toward the  $z$  axis is then simulated and the effective damping can be extracted from the magnetization trace by fitting Eq. (9) with the simulation results. From the above equation, we define the coefficients  $k_1 = \alpha\gamma B/1 + \alpha^2$  and  $k_2 = \gamma B/1 + \alpha^2$ , where the effective damping constant can be expressed in terms of  $k_1$  and  $k_2$ , as  $\alpha_{\text{eff}} = k_1/k_2$ .

We first study the magnetization dynamics of a Co-Fe-B system with a thickness of 2 nm at 300 K as an example simulation to calculate the effective damping constant. After thermal equilibration, all of the spins are coherently rotated by an angle of  $30^\circ$  and the system is then allowed to relax back to equilibrium under a 10 T applied field. The dynamics of the  $y$  and  $z$  components of the magnetization obtained from the atomistic model are shown in Fig. 3(a). Subsequently, the magnetization components are fitted by using Eq. (9), where  $k_1$  and  $k_2$  are coefficients used to match the dynamics of the magnetization. We consequently obtain the effective damping constant for this case,  $\alpha_{\text{eff}} = 0.0113$ , arising from the contribution of magnetic damping from both the bulk layer and the interfacial layer, showing a small enhancement over the expected value of  $\alpha = 0.0107$  for this thickness. Now, we turn to the thickness dependence of the effective damping constant at 300 K by varying the Co-Fe-B film thickness up to 20 nm to make a direct comparison with the experimental measurements in Ref. [1]. As demonstrated in Fig. 3(b), the value of the effective damping can be explained in three regions. The magnitude of  $\alpha$  decreases steeply with increasing thickness of the Co-Fe-B film below 2 nm. For a thickness of 2–5 nm, the increase in the Co-Fe-B thickness leads to a linear decrease in the damping constant. However, in the case of Co-Fe-B thicknesses above 5 nm, the magnitude of  $\alpha$  becomes nearly constant and close to the damping constant of the bulk layer,  $\alpha = 0.003$ . This can be understood as follows. For thin films, the interface contribution is the dominant contribution to the effective damping and due to the small finite thickness the dynamics are essentially coherent within the film thickness. For thicker films, the enhancement of the effective damping constant is governed by the bulk damping constant as some degree of incoherent relaxation is allowed, so that the spins far from the interface relax more slowly. We note that the origin of this effect is the finite thickness of the film rather than temperature effects, as we also observe the same behavior at 0 K. As demonstrated in the inset of Fig. 3(b), we also

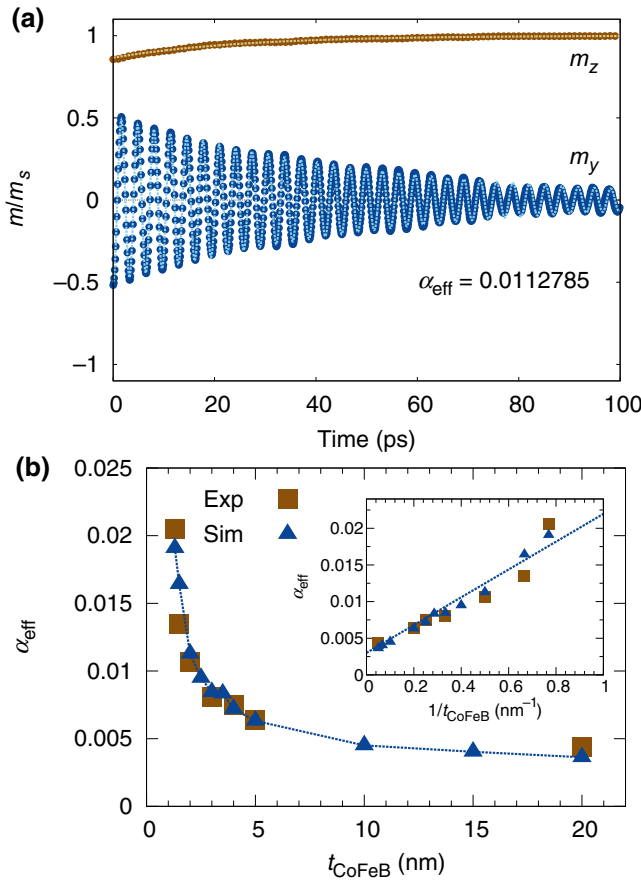


FIG. 3. (a) The time evolution of the magnetization component of the Co-Fe-B system with a thickness of 2 nm at 300 K after a  $30^\circ$  rotation of the equilibrated spin configuration. The points show the analytical magnetization components and the dashed lines represent the simulated magnetization. (b) A comparison of the effective Gilbert damping constant of the Co-Fe-B system with different thicknesses at 300 K, obtained from simulations and experiments in Ref. [1]: the line is a linear fit on  $1/t_{\text{CoFeB}}$ ,  $\alpha_{\text{eff}} = 0.003 + 0.0189677/t_{\text{CoFeB}}$ . The simulated thickness dependence of the effective damping quantitatively agrees with the experimental data.

observe a variation of the effective damping as a function of  $1/t_{\text{CoFeB}}$ . The linear relationship between  $\alpha$  and  $1/t_{\text{CoFeB}}$  is not observed for very thin films, where some nonlinear behavior is seen. This is likely due to additional thermal fluctuations at small sizes giving an additional contribution to the damping from thermal-spin waves. Our results are in excellent agreement with the experiments in Ref. [1], confirming the validity of the magnetic parameters of the Co-Fe-B/MgO system used in the atomistic model to calculate the effective damping constant.

### B. The temperature dependence of the effective damping constant

So far, we have considered the magnetic properties of the Co-Fe-B/MgO structure and confirmed the

applicability of the atomistic model for effective damping calculation by making a direct comparison between simulation and experimental data. We now consider the influence of temperature on the effective damping constant of the Co-Fe-B/MgO system with different thicknesses ranging from 2 nm to 20 nm. To evaluate the effective damping constant, we perform atomistic calculations including the effect of temperature-induced thermal-spin fluctuations in the range 0–400 K. Due to the small size of the system, we perform 30 independent relaxation simulations for each thickness and with different thermal fluctuations. Each simulation uses a different sequence of pseudorandom numbers for the stochastic thermal field in the atomistic model, thereby representing a different statistical sample.

The simulated temperature dependence of the mean effective damping parameter for different thicknesses is shown in Fig. 4(a). For each thickness, we find that

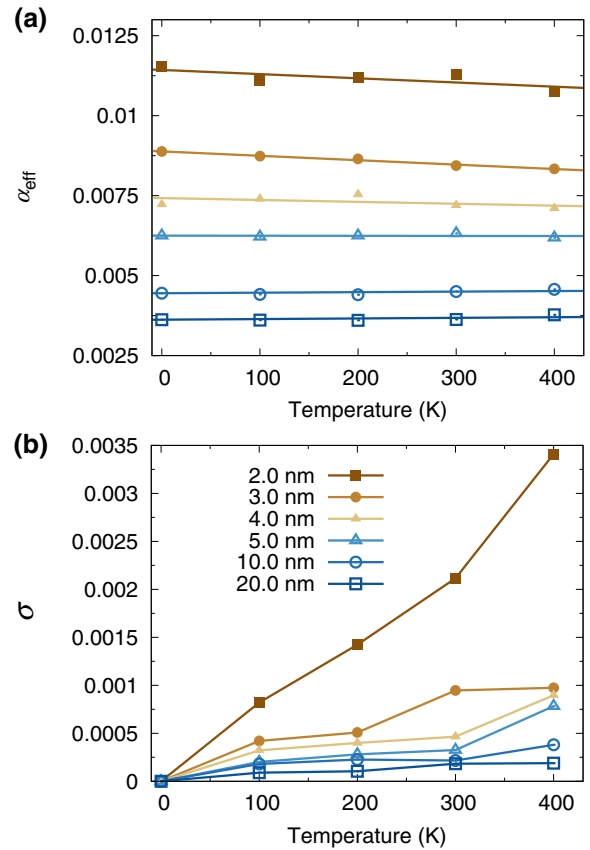


FIG. 4. (a) The simulated temperature dependence of the mean effective Gilbert damping constant of the Co-Fe-B/MgO structure for different thicknesses extracted from 20 stochastic simulation runs. The data show a weak temperature dependence and strong thickness dependence. (b) The temperature dependence of the standard deviation ( $\sigma$ ) of the distribution of the simulated Gilbert damping constants as a function of the film thickness. The data show a strong finite size dependence on the distribution of the Gilbert damping parameter, with a 30% deviation for 2-nm-thick films at 400 K.

temperature has a weak influence on the mean effective damping parameter and that it is essentially constant in the temperature range 0–400 K. This observation is consistent with experimental studies [33,34]. From our statistical samples of the relaxation dynamics, we fit a Gaussian distribution to determine the scatter in the effective damping parameter. The standard deviation of the effective damping distribution as a function of the film thickness and temperature is plotted in Fig. 4(b). Here, we find a very strong thickness and temperature dependence of the distribution. This effect is essentially a statistical thermal contribution to the damping due to the finite thickness of the film. As the film thickness is reduced, the thermal fluctuations become much more important to the dynamics and lead to a large deviation in the effective damping. For films thinner than 2 nm, the data become noisier due to the larger thermal fluctuations at elevated temperatures and so the fitting to obtain the Gilbert damping is challenging. However, we expect that the trend of an increasing distribution of the

damping with decreasing film thickness will lead to a much stronger effect at the 1.0–1.5 nm Co-Fe-B thicknesses used in devices.

To gain further insight, we show the simulated relaxation dynamics for the 2 nm film thickness at 400 K and the fitted damping parameters in Fig. 5. The data show a clear difference in the effective damping owing solely to statistical variations of the thermal fluctuations at small sizes, in this extreme case showing a factor of 2 change in the effective damping of the system. The system in Fig. 5 is identical in every respect. This is a previously unseen phenomenon; the Gilbert damping is usually assumed to be a material constant. Indeed, the average Gilbert damping shown in Fig. 4 is essentially independent of temperature. Our findings are of relevance for nanoscale spintronic devices, where reliable operation depends on tight control of the material properties and dynamic response. The purely thermal origin of this statistical variation of the damping is intrinsic to the finite system size and unavoidable, and presents a potential challenge for devices operating at high frequencies in excess of 1 GHz.

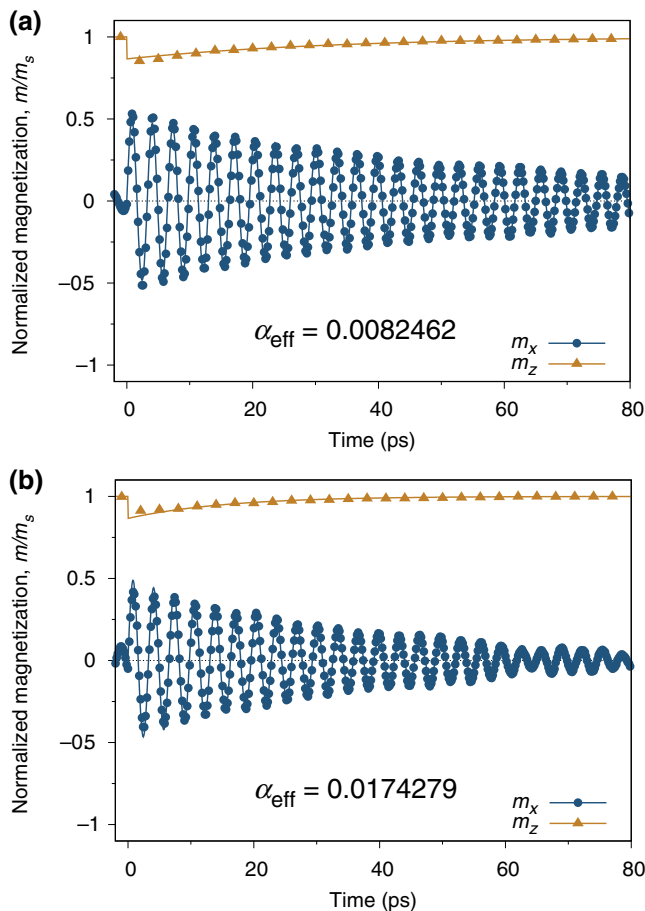


FIG. 5. The simulated relaxation dynamics (points) for a 2-nm-thick Co-Fe-B/MgO film at  $T = 400$  K. For different random thermal fluctuations, simulated through a different pseudorandom sequence, the same system displays (a) low and (b) high values of the effective Gilbert damping constant (fits shown by lines).

#### IV. CONCLUSIONS

In summary, we investigate the thickness and temperature dependence of the effective Gilbert damping parameter of the Co-Fe-B/MgO bilayer, which is a promising candidate material for spintronic devices and spin-based logic systems. The system is modeled considering a high-anisotropy high-Gilbert-damping monolayer in contact with the MgO layer, coupled to a low-damping low-anisotropy bulk layer away from the interface. We find a strong thickness dependence of the effective damping, in agreement with experiment, and an imperceptible temperature dependence of the mean effective damping in the temperature range 0–400 K. We note that the parameters in our model are only effective in that they include the role of the specific sample defects and disorder. Surprisingly, we find the existence of a strong statistical variation of the Gilbert damping for finite-size systems owing to random thermal fluctuations. This intrinsic thermal contribution to the dynamics of the system will need to be considered for high-speed spintronic devices operating at frequencies of 1 GHz or more. The random fluctuations may also partially explain the observed statistical variations of the reversal in pulsed STT switching [35,36]. Here, we only consider the isotropic contribution to the damping tensor but simulations of larger sample sizes and nanoscale devices would allow natural magnetic inhomogeneities to appear, which could enable a direct calculation of the Gilbert damping tensor and will be the subject of future work.

#### ACKNOWLEDGMENTS

This work was supported by the Samsung Global MRAM Innovation Program. S.S. would like to acknowledge

Ph.D. funding from Samsung Electronics. P.C. and J.C. gratefully acknowledge the funding from Mahasarakham University and Thailand Research Fund under Grant No. MRG6080048. This work made use of the facilities of the N8 HPC Centre of Excellence, provided and funded by the N8 consortium and EPSRC (Grant No. EP/K000225/1).

- 
- [1] S. Ikeda, K. Miura, H. Yamamoto, K. Mizunuma, H. D. Gan, M. Endo, S. Kanai, J. Hayakawa, F. Matsukura, and H. Ohno, A perpendicular-anisotropy CoFeB-MgO magnetic tunnel junction, *Nat. Mater.* **9**, 721 (2010).
- [2] Qiang Hao and Gang Xiao, Giant Spin Hall Effect and Switching Induced by Spin-Transfer Torque in a W/Co<sub>40</sub>Fe<sub>40</sub>B<sub>20</sub>/MgO Structure with Perpendicular Magnetic Anisotropy, *Phys. Rev. Appl.* **3**, 034009 (2015).
- [3] Atsushi Okada, Shikun He, Bo Gu, Shun Kanai, Anjan Soumyanarayanan, Sze Ter Lim, Michael Tran, Michiyasu Mori, Sadamichi Maekawa, Fumihiro Matsukura, Hideo Ohno, and Christos Panagopoulos, Magnetization dynamics and its scattering mechanism in thin CoFeB films with interfacial anisotropy, *Proc. Natl. Acad. Sci.* **114**, 3815 (2017).
- [4] Satoshi Iihama, Shigemi Mizukami, Hiroshi Naganuma, Mikihiko Oogane, Yasuo Ando, and Terunobu Miyazaki, Gilbert damping constants of Ta/CoFeB/MgO(Ta) thin films measured by optical detection of precessional magnetization dynamics, *Phys. Rev. B* **89**, 174416 (2014).
- [5] A. Conca, J. Greser, T. Sebastian, S. Klingler, B. Oby, B. Leven, and B. Hillebrands, Low spin-wave damping in amorphous Co<sub>40</sub>Fe<sub>40</sub>B<sub>20</sub> thin films, *J. Appl. Phys.* **113**, 213909 (2013).
- [6] Xiaoyong Liu, Wenzhe Zhang, Matthew J. Carter, and Gang Xiao, Ferromagnetic resonance and damping properties of CoFeB thin films as free layers in MgO-based magnetic tunnel junctions, *J. Appl. Phys.* **110**, 033910 (2011).
- [7] S. Mizukami, F. Wu, A. Sakuma, J. Walowski, D. Watanabe, T. Kubota, X. Zhang, H. Naganuma, M. Oogane, Y. Ando *et al.*, Long-Lived Ultrafast Spin Precession in Manganese Alloys Films with a Large Perpendicular Magnetic Anisotropy, *Phys. Rev. Lett.* **106**, 117201 (2011).
- [8] Richard F. L. Evans, Weijia J. Fan, Phanwadee Chureemart, Thomas A. Ostler, Matthew O. A. Ellis, and Roy W. Chantrell, Atomistic spin model simulations of magnetic nanomaterials, *J. Phys.: Condens. Matter* **26**, 103202 (2014).
- [9] A. V. Khvalkovskiy, D. Apalkov, S. Watts, R. Chepulskii, R. S. Beach, A. Ong, X. Tang, A. Driskill-Smith, W. H. Butler, P. B. Visscher *et al.*, Basic principles of STT MRAM cell operation in memory arrays, *J. Phys. D: Appl. Phys.* **46**, 74001 (2013).
- [10] G. D. Fuchs, J. C. Sankey, V. S. Pribyag, L. Qian, P. M. Braganca, A. G. F. Garcia, E. M. Ryan, Zhi-Pan Li, O. Ozatay, D. C. Ralph *et al.*, Spin-torque ferromagnetic resonance measurements of damping in nanomagnets, arXiv preprint cond-mat/0703577 (2007).
- [11] Satoshi Iihama, Shigemi Mizukami, Hiroshi Naganuma, Mikihiko Oogane, Yasuo Ando, and Terunobu Miyazaki, Gilbert damping constants of Ta/CoFeB/MgO (Ta) thin films measured by optical detection of precessional magnetization dynamics, *Phys. Rev. B* **89**, 174416 (2014).
- [12] S. Mizukami, S. Iihama, N. Inami, T. Hiratsuka, G. Kim, H. Naganuma, M. Oogane, and Y. Ando, Fast magnetization precession observed in L1<sub>0</sub>-FePt epitaxial thin film, *Appl. Phys. Lett.* **98**, 052501 (2011).
- [13] Satoshi Iihama, Qinli Ma, Takahide Kubota, Shigemi Mizukami, Yasuo Ando, and Terunobu Miyazaki, Damping of magnetization precession in perpendicularly magnetized CoFeB alloy thin films, *Appl. Phys. Express* **5**, 083001 (2012).
- [14] Ehsan Barati and Marek Cinal, Quantum mechanism of nonlocal Gilbert damping in magnetic trilayers, *Phys. Rev. B* **91**, 214435 (2015).
- [15] Yi Liu, Zhe Yuan, R. J. H. Wesselink, Anton A. Starikov, and Paul J. Kelly, Interface Enhancement of Gilbert Damping from First Principles, *Phys. Rev. Lett.* **113**, 207202 (2014).
- [16] Fan Pan, Jonathan Chico, Johan Hellsvik, Anna Delin, Anders Bergman, and Lars Bergqvist, Systematic study of magnetodynamic properties at finite temperatures in doped permalloy from first-principles calculations, *Phys. Rev. B* **94**, 214410 (2016).
- [17] Neil Smith, Tensor damping in metallic magnetic multilayers, *Phys. Rev. B* **80**, 064412 (2009).
- [18] Danny Thonig, Yaroslav Kvashnin, Olle Eriksson, and Manuel Pereiro, Nonlocal Gilbert damping tensor within the torque-torque correlation model, *Phys. Rev. Mater.* **2**, 013801 (2018).
- [19] Richard F. L. Evans, Sarah Jenkins, Andrea Meo, Matt Ellis, O. D. Arbeláez-Echeverri, Samuel Morris, Rory Pond, Razvan Ababei, Sam Westmoreland, and Phanwadee Chureemart, *Richard-Evans/vampire* (2019); VAMPIRE software package v5.0 also available from <https://vampire.york.ac.uk>.
- [20] M. O. A. Ellis, T. A. Ostler, and R. W. Chantrell, Classical spin model of the relaxation dynamics of rare-earth doped permalloy, *Phys. Rev. B* **86**, 174418 (2012).
- [21] G. J. Bowden, G. B. G. Stenning, and G. van der Laan, Inter and intra macro-cell model for point dipole-dipole energy calculations, *J. Phys.: Condens. Matter* **28**, 066001 (2016).
- [22] William Fuller Brown, Thermal fluctuations of a single-domain particle, *Phys. Rev.* **130**, 1677 (1963).
- [23] A. Lyberatos, D. V. Berkov, and R. W. Chantrell, A method for the numerical simulation of the thermal magnetization fluctuations in micromagnetics, *J. Phys.: Condens. Matter* **5**, 8911 (1993).
- [24] A. Lyberatos and R. W. Chantrell, Thermal fluctuations in a pair of magnetostatically coupled particles, *J. Appl. Phys.* **73**, 6501 (1993).
- [25] José Luis Garcia-Palacios and Francisco J. Lázaro, Langevin-dynamics study of the dynamical properties of small magnetic particles, *Phys. Rev. B* **58**, 14937 (1998).
- [26] O. Chubykalo, J. D. Hannay, M. Wongsam, R. W. Chantrell, and J. M. Gonzalez, Langevin dynamic simulation of spin waves in a micromagnetic model, *Phys. Rev. B* **65**, 184428 (2002).
- [27] William T. Coffey and Yuri P. Kalmykov, Thermal fluctuations of magnetic nanoparticles: Fifty years after Brown, *J. Appl. Phys.* **112**, 121301 (2012).



- [28] Andrea Meo, Phanwadee Chureemart, Shuxia Wang, Roman Chepulskey, Dmytro Apalkov, Roy W. Chantrell, and Richard F. L. Evans, Thermally nucleated magnetic reversal in CoFeB/MgO nanodots, *Sci. Rep.* **7**, 16729 (2017).
- [29] H. Sato, P. Chureemart, F. Matsukura, R. W. Chantrell, H. Ohno, and R. F. L. Evans, Temperature-dependent properties of CoFeB/MgO thin films: Experiments versus simulations, *Phys. Rev. B* **98**, 214428 (2018).
- [30] Ramón Cuadrado, László Oroszlány, András Deák, Thomas A. Ostler, Andrea Meo, Roman V. Chepulskey, Dmytro Apalkov, Richard F. L. Evans, László Szunyogh, and Roy W. Chantrell, Site-Resolved Contributions to the Magnetic-Anisotropy Energy and Complex Spin Structure of Fe/MgO Sandwiches, *Phys. Rev. Appl.* **9**, 054048 (2018).
- [31] P. He, X. Ma, J. W. Zhang, H. B. Zhao, G. Lpke, Z. Shi, and S. M. Zhou, Quadratic Scaling of Intrinsic Gilbert Damping with Spin-Orbital Coupling in  $L1_0$  FePdPt Films: Experiments and *Ab Initio* Calculations, *Phys. Rev. Lett.* **110**, 077203 (2013).
- [32] Chi-Feng Pai, Yongxi Ou, D. C. Ralph, and R. A. Buhrman, Dependence of the efficiency of spin Hall torque on the transparency of Pt/ferromagnetic layer interfaces, arXiv preprint arXiv:1411.3379 (2014).
- [33] Guangduo Lu, Xiufeng Huang, Shuaiwei Fan, Weiwei Ling, Min Liu, Jie Li, Lichuan Jin, and Liqing Pan, Temperature- and thickness-dependent dynamic magnetic properties of sputtered CoFeB/Ta bilayer films, *J. Alloys. Compd.* **753**, 475 (2018).
- [34] Xiao Wang, Jiafeng Feng, Peng Guo, H. X. Wei, X. F. Han, B. Fang, and Z. M. Zeng, Temperature dependence of spin-torque driven ferromagnetic resonance in MgO-based magnetic tunnel junction with a perpendicularly free layer, *J. Magn. Magn. Mater.* **443**, 239 (2017).
- [35] Christian Hahn, Georg Wolf, Bartek Kardasz, Steve Watts, Mustafa Pinarbasi, and Andrew D. Kent, Time-resolved studies of the spin-transfer reversal mechanism in perpendicularly magnetized magnetic tunnel junctions, *Phys. Rev. B* **94**, 214432 (2016).
- [36] T. Devolder, Joo-Von Kim, F. Garcia-Sanchez, J. Swerts, W. Kim, S. Couet, G. Kar, and A. Furnemont, Time-resolved spin-torque switching in MgO-based perpendicularly magnetized tunnel junctions, *Phys. Rev. B* **93**, 024420 (2016).